Uncertainties propagation in the UAM numerical rod ejection benchmark

Antonio Sargeni, Fabrice Fouet, Evgeny Ivanov, Pierre Probst

UNCERTAINTIES PROPAGATION IN THE UAM NUMERICAL ROD EJECTION BENCHMARK

A. Sargeni[1], F. Fouet[1], E. Ivanov[1], P. Probst[1]

[1]IRSN
BP 17 – 92262 Fontenay aux Roses Cedex - France

antonio.sargeni@irsn.fr, fabrice.fouet@irsn.fr, evgeny.ivanov@irsn.fr, pierre.probst@irsn.fr

ABSTRACT

This paper presents the execution and the results of a rod ejection benchmark inspired by the UAM benchmarks II-2b: cross sections uncertainties propagation during a rod ejection transient in a mini-core (3x3 PWR-type assemblies), without feedback. Performing transient computations in two groups time-dependent neutron diffusion approximation while starting from a steady-state power of 0.1409 MW, we obtained a mean power peak around 0.25 MW with a standard deviation of, nearly, 1.5%. The time-dependent standard deviation curve follows the time-dependent mean power curve and the relative standard deviation, in a percentage of the mean power, increases with the mean power peak value. We found, too, that the first group diffusion coefficient and the first group absorption cross section are, practically, the only contributors to the total power peak variance. Drawbacks and findings from the exercise provide essential input for uncertainty propagation in a further multi-physics simulation of a postulated rod ejection accident.

KEYWORDS: Uncertainties propagation, rod ejection, UAM

1. INTRODUCTION

Nuclear engineering and scientific communities expressing their continued interest to a comprehensive modeling of nuclear power systems used to pay particular attention to a confidence metrics for best estimate tools and their uncertainties within relevant design and safety assessment frameworks (K. Ivanov 2019). This is why the OECD-NEA Nuclear Science Committee (NSC) initiated around ten years ago a deep multi-lateral relevant discussion followed by an establishment of a dedicated Expert Group (EG) on 'Uncertainty Analysis Modelling' (UAM). The 'Expert Group on Uncertainty Analysis Modelling' (EGUAM) nowadays is a part of the NSC 'Working Party on Scientific Issues on Reactor Systems' (WPRS) to developing and performing a set of benchmark studies on uncertainties propagation through all design and assessment phases of Light Water Reactor (LWR) presenting all results in a form of UAM-LWR benchmarks (Hou et al., 2017) which comprises the following steps:

1) subdivision of the systems/scenarios in some steps (exercises),
2) clear identification of the inputs, outputs and the hypotheses for each step,
3) evaluation of uncertainties for each step and
4) propagation of the uncertainties along with the entire design studies and through all scenarios.

This UAM-LWR approach has been translated into nine exercises that mix experimental data and numerical benchmarks. They went from a neutronic phase to a core behavior phase and, then, to a system phase as follows.

The neutronic phase is composed of the exercises:

- I-1, derivation of the multi-group microscopic cross-section libraries,
- I-2, derivation of the few-group macroscopic cross-section libraries,
- I-3, criticality stand-alone calculations with confidence bounds.

The core phase is composed of the exercises

- II-1, fuel thermal properties relevant for transient performance,
- II-2, neutron kinetics stand-alone performance,
- II-3, thermal hydraulic fuel bundle performance.

The system phase is composed of the exercises

- III-1, coupled neutronic/thermal hydraulic core performance,
- III-2, thermal hydraulics system performance,
- III-3, coupled neutronic kinetics/thermal-hydraulics core/system performance.

The IRSN (the French Institute for the Radiological Protection and Nuclear Safety) according to its main mission of technical support to the French Authority should be at the state-of-the-art of scientific knowledge. The uncertainties quantification in the field of interest has been considered as one of the most challengeable research areas that could contribute to better understanding the potential needs of "tomorrow's expertise". For all these reasons, aiming to maintain the competence, IRSN takes part in the UAM-LWR activity both as a benchmark co-author and as a researcher selecting some cases for deeper elaborations. One of these cases, namely related to core behavior exercise II-2b (Hou et al., 2017) presents a numerical rod ejection benchmark on a mini-core with PWR-type assemblies, without feedback. In our opinion, the exercise II-2b could be useful to highlight the impacts of the cross sections uncertainties on an analysis of a practical safety case driven by a rod ejection transient. It could give valuable inputs for further phases of the UAM-LWR benchmark and for further elaboration of error propagation techniques. The approach applied in the exercise was to do numerous transients computing the mean power and the standard deviation. Each transient has been modeled with a given set of cross sections (XS) and kinetic parameters generated by a random perturbation of nuclear data assuming a normal distribution of nuclear data uncertainties. The standard deviations of XS were derived from the library supplied by the UAM team (UAM-XS).
One should note that the subjects of reactivity insertion accidents, as such, have been well-described in numerous publications. For example, (Barre et al, 2010) and (Hursin et al, 2013) provide a general overview of fuel safety in a different scenario including Reactivity Insertion Accidents (RIA) caused by rod ejection. Among them, one could see advanced analysis of uncertainty propagation through such transients (Miglierini et al, 2019), (da Cruz et al, 2014) and (Diamond et al, 2000).

Being aware of the worldwide trends and of these publications as well, we focused on our work on an analysis of a methodology and practice of propagation of nuclear data uncertainties.

A part of the results presented here has recently been presented at the PHYSOR Conference (Sargeni et al, 2018). This paper gives a complete presentation and a deeper discussion of our results.

In the following, after the benchmark description (chapter 2), we present the results (chapter 3). Chapter 4 is dedicated to some sensitivities analysis and chapter 5 contains some comments about all the results presented in this paper.

2. BENCHMARK DESCRIPTION

The rod ejection is executed in a mini-core (Hou et al., 2017), (Avramova et al, 2020), (Bratton et al, 2014) composed by a 3x3 cluster of fuel PWR-type assemblies, surrounded by a reflector. Side, top, and bottom reflectors are identical. The reflector model is a 1D: fuel (21.6 cm), water gap (0.21 cm), stainless steel shroud (1.91 cm) and water (19.521 cm). The active core height is 365.76 cm, side and axial reflectors are 21 cm tall. The assemblies (Figure 1) have 15x15 UO2 pins (U235 enrichment 4.12 w/o) with 4 gadolinium pins (2% w/o):

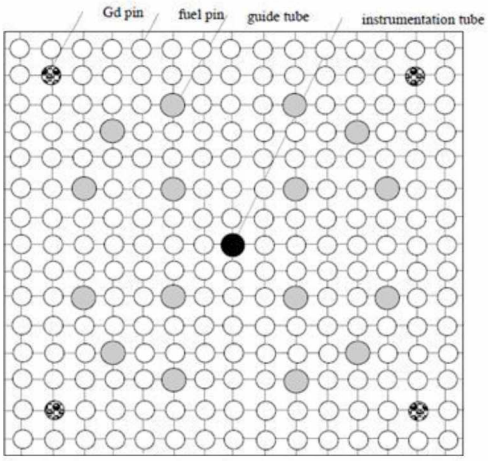

Figure 1: TMI Assembly (Bratton et al, 2014)

The fuel rod pitch is 1.443 cm and the fuel + clad diameter is 1.092 cm. The central assembly has a control rod ('R' in Figure 1) and the 8 others without control rod ('U', in Figure 2):

Reflector	Reflector	Reflector	Reflector	Reflector
Reflector	U	U	U	Reflector
Reflector	U	R	U	Reflector
Reflector	U	U	U	Reflector
Reflector	Reflector	Reflector	Reflector	Reflector

Figure 2: mini-core (Bratton et al, 2014)

The central control rod (CR) is composed of 14 AIC (Silver-Indium-Cadmium) pins. In our calculations, the AIC pin diameter is taken equal to French PWR AIC pins diameter and it is slightly

smaller than the diameter specified in the benchmark. The benchmark had no specifications about the AIC' density, we have taken the AIC density of a French PWR. All the fuel assemblies are composed of fresh fuel; i.e. zero MWd/tHM exposure. The mini-core is in a Hot Zero Power (HZP) state, its state is summarized in Table 1:

Table 1: HZP mini-core parameters (Bratton et al, 2014)

Parameter	**Value**
Mean fuel temperature	551 °K
Mean cladding temperature	551 °K
Mean coolant temperature	551 °K
Mean coolant density	0.76846 g/cm3
Mini-core Power	0.1409 MW

It is important to note that, due to the small core power value, the temperatures and coolant density distributions were, practically, uniform.

The control rod in central assembly is fully inserted at time 0 and ejected in 10 seconds over a distance equal to 12% (43.8912 cm) of the active core height (365.76 cm). It is then re-inserted in 20 seconds to its fully inserted position. The transient had to be computed without feedback.

The benchmark specifications prescribe computing the mean values and the standard deviations for all given transients.

3. BENCHMARK EXECUTION AND RESULTS

Transient processes for mini-core have been simulated using HEMERA simulation chain (Dubois et al., 2012) that combines a full core 3D neutron diffusion two-group solver (group 1, fast, neutrons with energy > 0.625 meV; group 2, thermal, neutrons with energy < 0.625 meV) and a mono-phasic thermal hydraulic module. Over here we used the only CRONOS (Lautard et al., 1990), the time-depended neutronics code instead of entire calculation chain. The cross sections (XS) uncertainties were propagated using brute-force technique, i.e. performing numerous launches of the code with initial data (XS libraries) that were pre-generated using randomly perturbed parameters. Post-treatment applied then provided relevant mean values and standard deviations.

3.1. A brief description of APOLLO2/CRONOS computation chain

As said, all transients have been executed using the in-house developed IRSN 3D calculation chain HEMERA and, in particular, its neutronic module CRONOS.

CRONOS is a finite difference, deterministic, 3D neutronic code. It computes few-group flux and power distributions in an entire core. Each mesh in CRONOS has uniformed cross section (XS) set parametrized versus fuel and coolant temperatures, moderator density, burn-up (zero exposure in our case), boron concentration and a height of control rod insertion.

The cross-section library is generated using the APOLLO2 code (Sanchez et al., 2010) which is a deterministic multi-group solver to model particle transport in a fuel assembly. Over here were collapsed XS using APOLLO2 with JEF2.2 nuclear data library and in an exact fuel pins and guide tubes geometry.

The core was modeled with 4 radial meshes by assemblies, 24 axial meshes in the active core (imposed by the benchmark) and 2 energy groups. The side, top, bottom reflectors assemblies had 4 radial and 24 axial meshes as well.

3.2. Cross Sections Uncertainty Treatment

In the preparation of data for the uncertainty sampling procedure, a normal distribution of changes in the initial nuclear data is assumed. The basic (mean) values were computed using APOLLO2, while relevant standard deviations were derived directly from the data distributed by the UAM-LWR team (UAM-XS, 2014) and computed with SCALE6.2b3 and the XS library ENDF-B.VII.

The XS have been modified within relevant intervals of uncertainties presuming the last ones normally distributed. The mean values of the XS were taken as non-perturbed ones, interpolated using CRONOS as mesh-wise matrices. The absolute values of the standard deviations were computed using the relative standard deviations provided in the UAM benchmark.

We used pre-evaluated relative standard deviations by the following reasons: 1) there is not yet in APOLLO2 a robust procedure to compute covariance matrices for a few group XS; 2) we tried keeping methodological affinity with other participants of UAM; and, last but not least, 3) it is well-known that Nuclear Data (ND) and their uncertainties have different nature being fundamentally independent[1] (M. Salvatores, 2014) and such use of different sources for ND and uncertainties would not compromise S/U analysis. The last one has been also supported by the comparisons performed years ago inside the IRSN (N. Leclaire, 2009), between APOLLO2 and SCALE6.1 and SCALE6.2b3, for k_{eff} and XS calculations.

We plan, in a next future, to calculate ourselves our covariance matrix as well as to replace so-called prior ones onto covariance matrices adjusted using GLLSM and relevant integral experimental data (M. Salvatores, 2014).

In each mesh, we modified 12 2-group XS (fast and thermal diffusion coefficients, absorption, production, fission, energy by fission), up and down scattering and 14 kinetics parameters - 6 delay neutrons fractions (hereinafter denoted as Beta N, N=1 to 6), 6 precursors decay constants (Lambda N, N=1 to 6), 2 1/v terms). All these modifications are computed once for each transient in its very beginning point.

3.3. Computation methodology

All computations have been executed with the following steps:

- A steady-state is computed:
  - Determination of a set of multiplicative coefficient following a normal probability law.
  - Computation of a cross section set by mesh. The multiplicative coefficients above are applied to each cross section and kinetic parameter.
  - Search for critical boron. This process is not linear: each new boron value modifies the cross sections value, which implies determining a new boron value and so on until convergence.
  - At the end, the steady state is critical and a 3D xenon distribution has been calculated.
- The transient begins. The steady-state xenon distribution is kept constant.

[1] It is true up to the very detail matters in ND libraries formats (not in ND, as such) and in a treatment of ND generating a few group XSs

With the choices above, each transient begins with a different boron concentration and with a slight different axial xenon distribution. The requirement to begin the transients starting from a critical state comes from a double reason:

a) To start the transient, CRONOS (Lautard et al, 1990) needs in initial precursors' concentrations. In our case they were computed at steady-state using the initial flux distribution. Of course, in case of non-zeroed reactivity the static flux means the only a mathematical abstraction making roughly approximate the initial, precursors' concentrations.
b) Starting a transient from a non-critical steady-state seems equivalent to an insertion of a step-wise initial reactivity. Of course, such non-physical model could perturb the power evolution during the rod-ejection transient.

3.4. Results

The main results of the benchmark are the core' mean power evolution and, above all, the dispersion of mean power. Statistical convergence has been achieved (i.e., when the curves of mean power and standard deviation become stable) after ~300 transient computations.

The core mean power and its upper and lower bounds are presented in Figures 3a and 3b. The mean power goes from 0.1409 MW to a maximum of, about, 0.25 MW. The upper and lower bounds have been obtained adding and subtracting to the mean power a percentage value equal to 3 standard deviations.

The computed standard deviation is time-dependent. It reaches its maximum value at the moment of the power peak; it decreases rapidly according to the power and; until the end of transient, is approximatively constant. This can be seen in Figures 3a (upper, mean and lower power transients, in MW) and 3b (mean power and relative standard deviation in a percentage of the mean power):

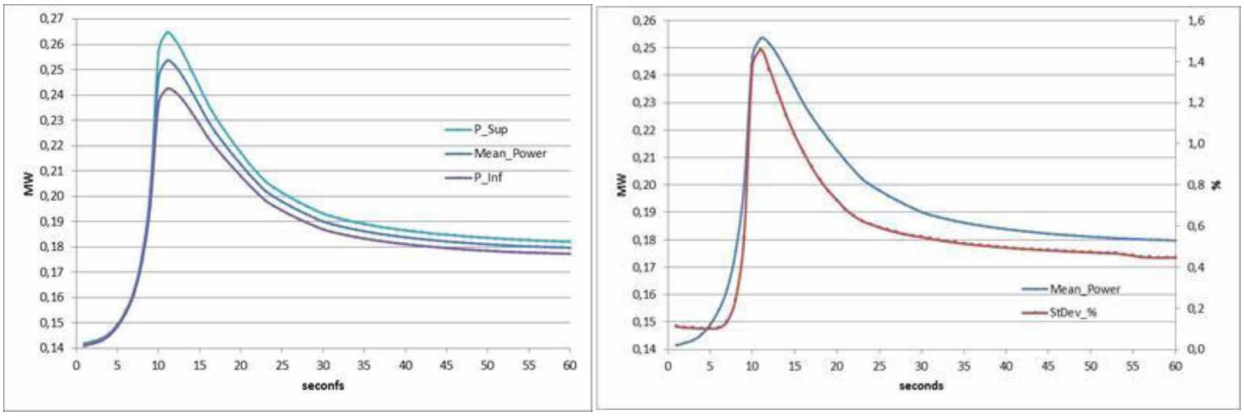

a b

Figure 3: a: Upper (P_Sup), Mean and Lower (P_Inf) Power (MW) (3 sigma) and b: Mean Power (MW) and Standard Deviation (% of the mean power) Transients

Some of the following observations could be noted concerning the results obtained in the simulations.

- The maximum standard deviation value is 1.45%. Although the value seems rather small we considered it as a reasonable one since the maximal deviation was in D1's while its worth was of 2.4%.
- The standard deviation curve follows the mean power distribution. In other words, it seems that the relative standard deviation, in a percentage of the mean power, depends on the level of the power and not only on the magnitude of uncertainty of the cross sections.

- Moreover, the curves seem to indicate the standard deviation grows faster than the mean power (see Figure 4a), where the derivatives of the mean power (in MW/s) and the relative standard deviation (in %/s) are depicted. The same curves, but normalized on maximum values, are depicted in Figure 4b.

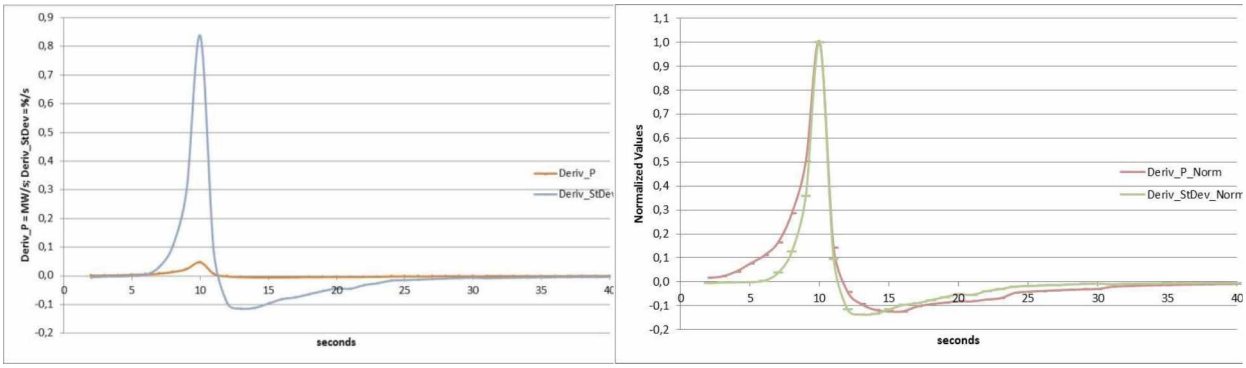

a b

Figure 4: Derivations of Power (a) and of Standard Deviations (b)

One may note that a recently published paper (Xinyi et al. 2017) demonstrates good agreement with what has been obtained in our work. The upper and lower limits of power transient uncertainty, found in the Xinyi paper, are qualitatively very similar to the results of this work (Figures 4).

4. SENSITIVITY ANALYSIS

To better understand the results, we asked ourselves some questions:

- We generated variations of XS presuming their normal distribution. In this case what would be a probability density distribution for the computed power peaks? Whether or not it depends on the height of the power peak?
- If a magnitude of the mean power peak changes whether or not the relative standard deviation remains constant or it changes as well?
- The standard deviation of each XS is different. What is its impact on a variance of the power peak?

Answering the question we had to run all the transients one more time, changing one cross section at the time comparing them with the variances.

- Are the cross section influences we found in the reference case (rod ejection equal to 12% of the active core height) always valid? Does it independent on the power peak?

The answer has been found by increasing the rod ejection distance from 12% to 15% of the active Core Height (CH). This enabled the power peak to go from 0.25 MW to 2.5 MW and, again by a modification of a cross section at the time, to obtain the answer.

4.1. Comments to the hypothesis of Normal Distribution of the Power Peaks

To check the 'normality' of the power peak distributions, we built a Cumulative Empirical Distribution Function (CEDF), where we arranged the power peak values in increasing order and given to each point the same weight (1/the number of cases). The degree of 'normality' or 'log-normality' of peak power distributions is given by the comparison between the theoretical CEDF and the CEDF obtained from the calculated peak values.

In the following, we present some curves at different times and for two rod ejections: the benchmark one (12% CH) and an ejection until 15% CH. Figure 5 presents the two CEDF at 1 second (curves are normalized, due to the strong difference in the power obtained for the two cases):

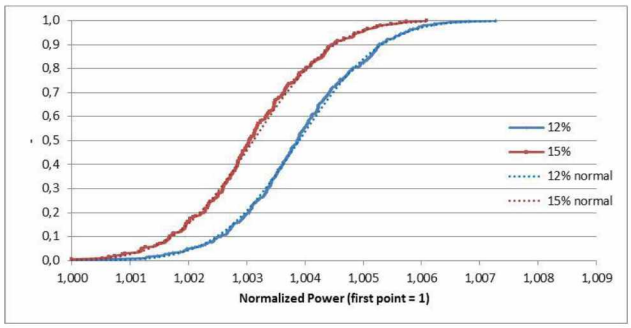

Figure 5: Cumulative Empirical Distribution Function – time = 1s

The two curves seem to be the expression of a variable following a normal distribution: they are very close to the theoretical, normal distributions.

At 11 seconds (very close to the mean power peak), the case 12% CH still follows a normal distribution , but for the case 15% CH (Figure 6) the situation is different

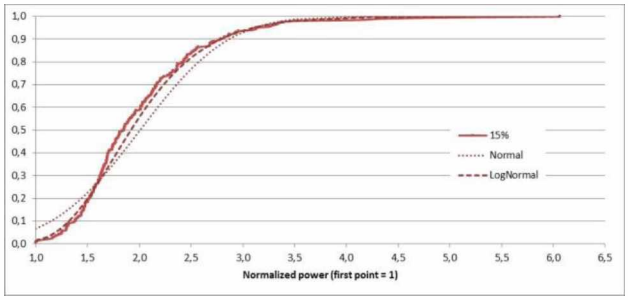

Figure 6: Cumulative Empirical Distribution Function – 15% CH - time = 11s

The curve of the 15% CH ejection seems, actually, closest to a log-normal distribution than to a normal one.

In conclusion, it seems that the normality of the cross sections standard deviations induces a normal distribution of the power peaks as well, provided that the power peak is not very far from the initial power. On the other hand, when the peak begins to be far from the initial power, the 'normality' tends to disappear in favor of a distribution similar to a log-normal distribution.

4.2. Variance Splitting

Next step of our study includes an analysis of the most impacting XS on the variance of the total power using two approaches: 1) a direct brute-force approach, where one or another element of few-group XS matrices were perturbed following a normal law and 2) an indirect one, where we pass through a surrogate model and a Sobol' analysis (Sobol', 1993).

4.2.1 Variance Splitting – Direct Approach

Since the standard deviation of each cross-section is different (including kinetic parameters), we assume that it is useful to determine which individual cross-section would have more or less influence on the variance of a peak power. To do this, we have perturbed each cross section and computing the variances of the correspondent power peaks for two cases of the rod ejections: 12% CH and 15 % CH.

The final results are depicted on Figure 7 which presents the ratio (in percentage) between the variance due to every section and the total variance (for 12% CH and 15% CH).

Honestly, it would worth comparing the main contributors obtained in different works in order to ensure a robustness of the given analysis. Although such kind of items was discussed on many workshops and conferences, we could not find many openly available relevant publications. One may mention (C. Mesado, et al, 2012) where authors computed uncertainties for the rod ejection transient presuming some feedback using Latin Hypercube and simple sampling techniques.

Despite the feedback exist over there and neglected in our case, the main contributors look similar to ours (see Figure 8) if consider the power and reactivity. Despite the notations are not completely the same, one can see that as in our case the fast diffusion group dominate over all other contributors. One should note that the only difference in a production component $\nu\Sigma_F$ appears because our colleagues included initial steady state in the consideration.

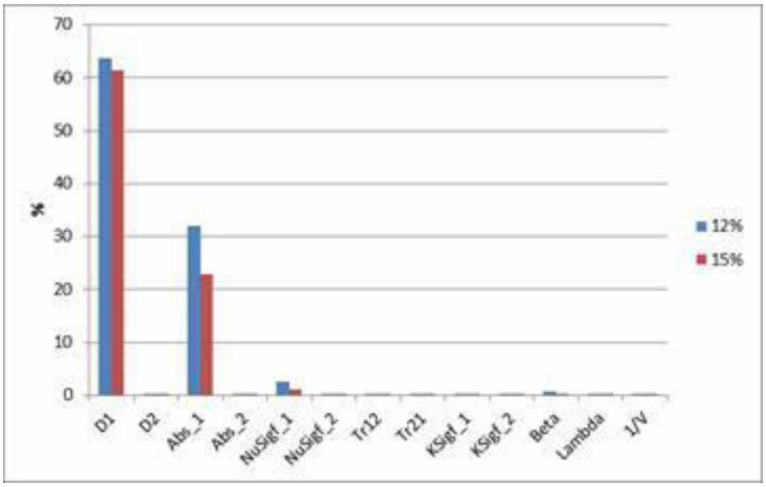

Figure 7: Power Peak XS Variance/Total Variance (this work)

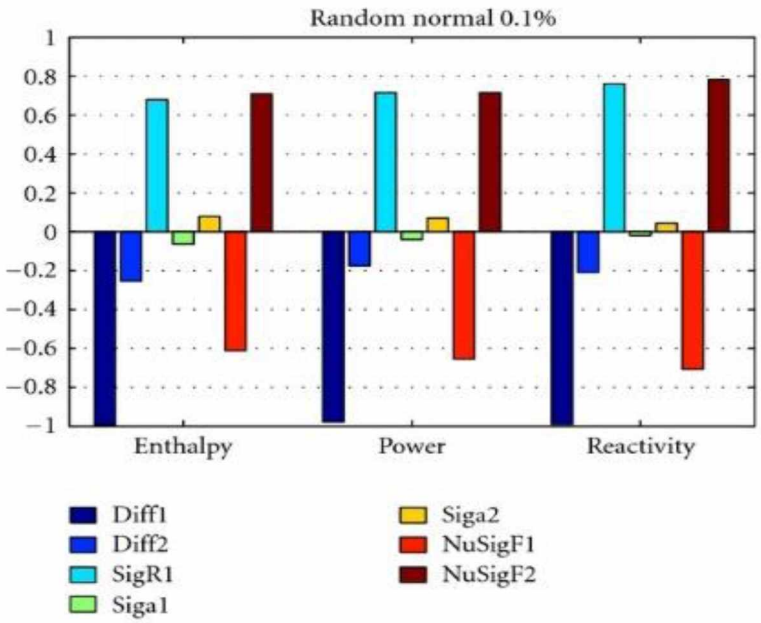

Figure 8. Major contributors in Enthalpy, Power and Reactivity according to (C. Mesado, et al, 2012)

One may do the following observations:

1) Whereas for the ejection up to 12% CH, the sum of the contributions gives almost 100, for the ejection of 15% CH we have only 85. A probable explication seems to be there are stronger non-linear effects in case 15% than in case 12%. And that the lack of linearity depends on the amplitude of the power peak: at 15% CH, the power peak 10 times greater than the peak at 12% CH;
2) In both cases, the most important contributions come from the fast diffusion coefficient (D1) and the fast absorption (Abs_1). The fast production cross section (NuSigf_1) gives a very small contribution and all the other cross sections are negligible. That does not seem correlated to the cross sections standard deviations. If we look at the cross sections standard deviations (represented in Figure 9), only for the fast diffusion coefficient, there is, simultaneously, a big standard deviation and a big contribution to the total variance. The scattering cross section from the group 1 to 2 (Scat_12) has a standard deviation bigger than the fast absorption one and its contribution is smaller.

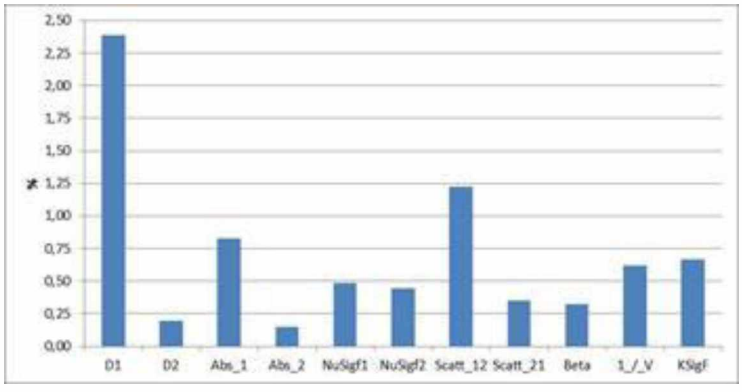

Figure 9: XS Standard Deviation at BU=0 MWd/tHM

An attempt to give to qualitatively explain n of this apparent contradiction is the following reasoning (the figures and data refer to the 12% CH ejection, but it is the same for the 15% CH case):

- There is a linear correlation between the dynamical rod worth (Rozon, 1992) at 10 seconds (when the rod is completely out) and the power peak. This relation can be seen in Figure 10 where we have plotted the maximum, dynamical rod worth versus the power peak:

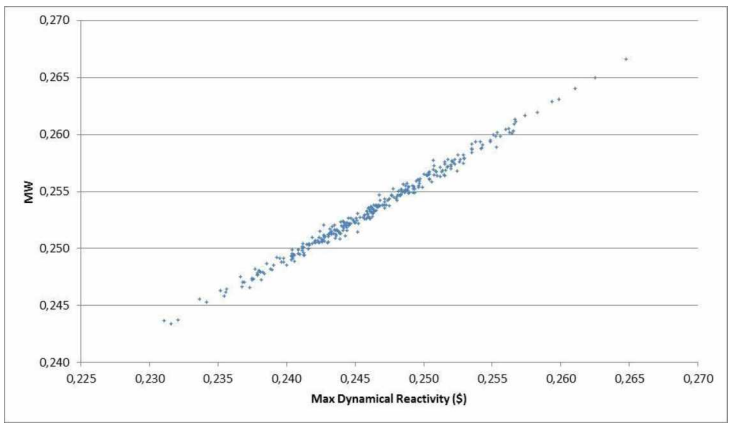

Figure 10: Power Peak vs Max Dynamical Reactivity

- There is a tight relationship between the dynamical (Rozon, 1992) and static reactivity. Figure 11 presents the two reactivities for the nominal transient :

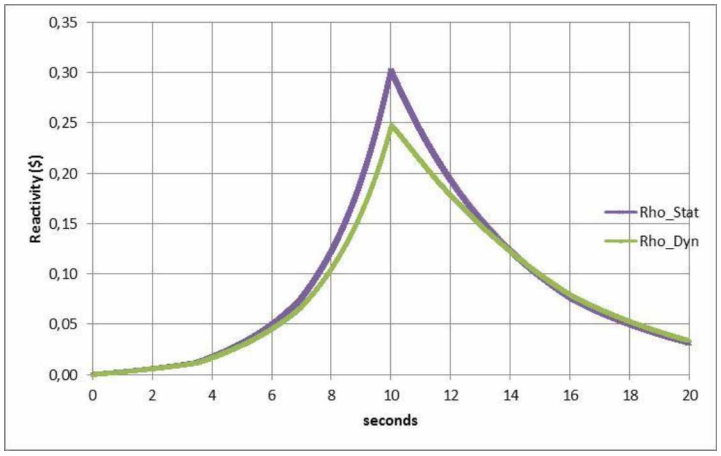

Figure 11: Static and Dynamical Reactivity – 12% CH

In particular, the time-dependent shapes of reactivity evolution are similar for the static and the dynamic ones, which demonstrate a consistency of the last one. It allows, in its order, to apply a sensitivity-uncertainty analysis in a traditional form since the reactivities' behaviors are similar, and dynamic rod worth and corresponded power peak have a linear link in between, and:

- The sensitivity coefficients were established as the ratio between a variation of the static rod worth (in $) over a cross section variation (in percentage). That gives an indicator of cross section importance for the rod worth.

- These sensitivity coefficients were multiplied by their standard deviations. In this way, it is easy to estimate the relative importance of the XS in terms of their contributions to the variability of the power peak.

Formally, the sensitivity coefficients are computed as a rod worth variation over a relative XS variation:

$$S_{XS} = \frac{(\rho_{OUT} - \rho_{IN})_{XS+\Delta XS} - (\rho_{OUT} - \rho_{IN})_{XS-\Delta XS}}{2\,\Delta XS/XS}, \quad (1)$$

Table 2 presents the sensitivity coefficients and the standard deviations for the first (fast) group of diffusion coefficient, absorption and down-scattering from the 1st to the 2nd groups where each ρ is given in \$ (reactivity divided by β_{eff}) and de-numerator of Eq. 1 equal 20%.

Table 2: Sensitivity Coefficients for the Rod Worth

XS	D1	Abs_1	Scattering 1->2
Sensitivity Coefficient ($/%XS)	-0,0033	+0,0061	-0,00051
Relative Standard Deviation (%)	2,386	0,825	1,222

Table 2 explains at the same time the reason why a contribution of D1 dominates over one of Abs_1 (see Figure 10) because the rod worth variability (sensitivity coefficient times standard deviation) is bigger for D1 than for Abs_1 as follows:

$$|S_{D1}| \times \sigma_{D1} = 0{,}00787 > |S_{Abs1}| \times \sigma_{Abs1=} = 0{,}00503 >> |S_{Tr12}| \times \sigma_{Tr12} = 0{,}000623, \quad (2)$$

To do a quick test about the validity of this conclusion, we divided the standard deviation of the fast diffusion coefficient, D1, (all the others one are kept constant) by two, which should reverse the D1 domination over Abs_1:

$$|S_{Abs1}| \times \sigma_{Abs1=} = 0{,}00503 > |S_{D1}| \times \sigma_{D1} = 0{,}00395. \quad (3)$$

If do so we could obtain the new variances (in percentage of the mean power peak) as they are presented in Table 3.

Table 3: Test Variances

D_1 Variance/Total Variance (%)	**Abs_1 Variance/Total Variance (%)**
36,5	66,5

According to the reasoning above, *we would say that the cross section influence on a power peak variation depends, at the same time, on its 'weight' (the sensitivity coefficient) and its uncertainty (the standard deviation)*.

As the final remark, we notice that this indicator is, in practice, a diagonal term of a 1st order variance estimated with the so-called 'sandwich rule' (Pusa, 2012).

4.2.2 Indirect Approach

To confirm and extend the variance analysis of the power peak, we used the next one two-steps approach based on a coarse selection of the most relevant input parameters (step 1) and a more precise evaluation of input parameters sensitivity indices performing a Sobol' formalism (step 2).

The Sobol' approach (Sobol', 1993) is a variance-based method for global sensitivity analysis, which decomposes the output variance into fractions which can be attributed to inputs or groups of inputs. It does not make any assumption on the model, compared to the linear model implicitly adopted for the direct approach, but requires the independence of the input parameters. The main idea of this approach is the decomposition of the function of the input parameters into summands of increasing dimensionality. In order to study the impact of the independent input parameters $x = (x_1, \dots, x_n)$ on the variance of the output $y = f(x_1, \dots, x_n)$, we can compare the variance of y namely $V(y)$ with the conditional variance of y with x_i fixed to its true value x_i^*, $V(y \mid x_i = x_i^*)$. Unfortunately, the true values of the input parameters are not generally known. Therefore, a solution consists in studying the conditional expectation $E[V(y \mid x_i)]$, whereby it is built into all possible values of x_i. The sensitivity indices of Sobol' are given by:

$$S_i = \frac{V[E(y \mid x_i)]}{V(y)} \qquad S_{ij} = \frac{V[E(y \mid x_i, x_j)]}{V(y)} - S_i - S_j \tag{4}$$

The first order sensitivity indices S_i measure the main effect of each input parameter x_i on the output y, or the fraction of variance of y due to the variance of x_i alone. The second order index S_{ij} expresses sensitivity of the model to the interaction between the variables x_i and x_j, (without the individual effects of x_i and x_j), and so on for the third, and higher order effects. Moreover, we define the total sensitivity index of variable x_i which is defined as the sum of its all sensitivity indices, its main effect as well as all the higher order effects in which this value appears:

$$S_{T_i} = S_i + \sum_{1 \le j \le n, j \ne i} S_{ij} + \dots + S_{1,2,\dots n} \tag{5}$$

Sobol' proposed to estimate the sensitivity indices by a method of Monte-Carlo.

However, this technique requires simulating many sets of parameters to propagate uncertainties correctly, which makes it a time-consuming approach. Therefore, we have replaced the direct computing by an approximate mathematical model, usually called a 'response surface' or a 'surrogate model'. The quality of the response surfaces depends on the choice of the experimental design. To construct our computer experiments and to generate a random sample of input parameter values, we have considered the Latin Hypercube Sampling (LHS) statistical method (Butler, 2001) with 300 design sets (each set consists of the 26 cross sections and kinetic parameters). This analysis was performed for both the 12% CH ejection case and for the 15% CH one.

Case of 12% CH ejection

To start with (step 1), we have defined a multiple linear regression (least-squares) between the power peak and the 26 input data and the 325 couples formed by all the 26 input data.

In this case of 12% CH ejection, we obtain a coefficient of determination (R^2) equal to 99.5%. That means nearly perfect linearity, as can be seen in Figure 12 where the points are well distributed around the first bisector, which shows that there is no prediction bias at all.

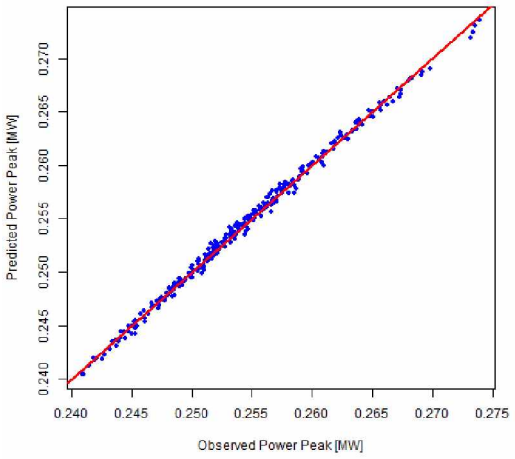

Figure 12: Comparison of the simulator outputs and the model predictions (ejection 12%)

The most significant regression coefficients are presented in Table 4. In this case (identical PDF[2] for each input parameter), these regression coefficients can be used to identify and to classify the most significant parameters. The two most relevant parameters are D1 and Abs_1. We should mention the rather significant influence due to their interaction (denoted D1:Abs_1 in Table 4) while all other interaction terms are far smaller.

Table 4: Regression coefficients by XS (case 12%)

Power Peak (at 11 sec.)	**Regression coefficients**
D1	-0.003060
Abs_1	+0.002250
NuSigf_1[3]	-0.000576
Beta 4	-0.000269
Scattering 1->2	-0.000205
Lambda 1	+0.000169
D1:Abs1	-0.000155
Lambda 4	+0.000138
Beta 3	-0.000133
Beta 2	-0.000104
Beta 5	-0.00007
NuSigf_2	-0.0000697
D1:NuSigf_1	0.0000322

From this first step, we have used the regression coefficients given above to select the 11 most probabilistically significant variables and, in the second step, we have applied them the Sobol' approach (with 100,000 Monte-Carlo iterations). The total Sobol' indices (S_{T_i}, equation (5)) are presented in Table 5, the first column. The power peak is sensitive essentially to the parameters D1 and Abs1, which explains abound 96% of the output total variance. Given the very high value of the determination coefficient (R^2=99.5%), the use of the Sobol' approach is unnecessary, but useful to confirm the linear regression results. The same results are obtained with the squared Standardized Regression Coefficients (SRC, Table 5, second column).

[2] Probability Density Function (PDF)

[3] Production XS for the 1st group

Table 5: Sobol' indices (total-order) and Standardized Regression Coefficients (SRC) for the most influent input parameters (case 12%)

Power Peak	Sobol' indices	SRC
D1	62,6	62,5
Abs1	33,7	33,7
NuSigf1	2,2	2,2
Beta 4	0,5	0,5
Scattering 1->2	0,3	0,3
Lambda 2	0,2	0,2
Lambda 4	0,1	0,1
Beta 2	0,1	0,1
Beta 3	0,1	0,1

We have carried out the same study considering as output parameters the power level at different times (between 3 and 60 seconds). We present in Figure 13 the temporal evolution of total-order sensitivity indices of Sobol' during the transient (only the most important ones are presented here). We can note that at the beginning of the transient (3s) before the power peak (11s), the most relevant parameters are Beta4 and Lambda2. These 2 parameters explain 62% of the power variance.

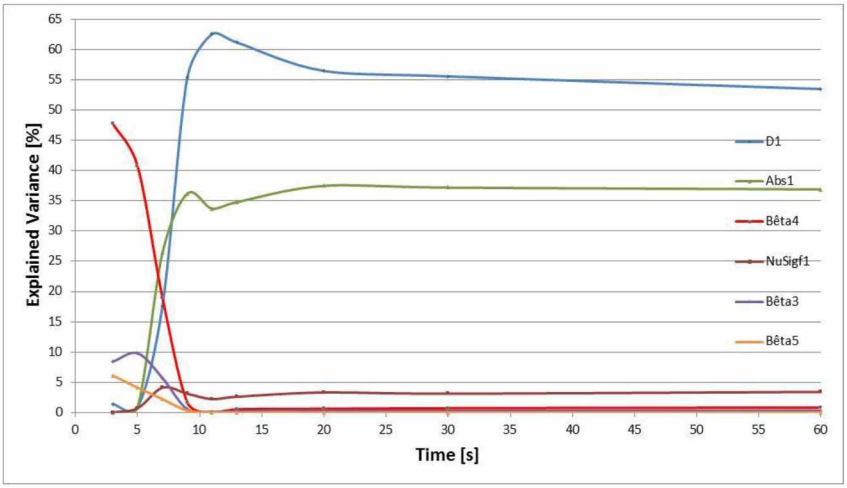

Figure 13: Sobol' indices time evolution (total-order) for each input parameters (12% CH)

Case of 15% CH ejection

Then, we have carried out the same study with a rod ejection up to 15% of the core height to analyze the sensitivity of the results to a biggest power peak. In this case, the construction of a response surface for modeling the power peak (reached at 12 s) with a multiple linear regression, leads to a coefficient of determination R^2 equal to 73%. Which indicates that the linearity hypothesis of the model is not verified (Figure 14):

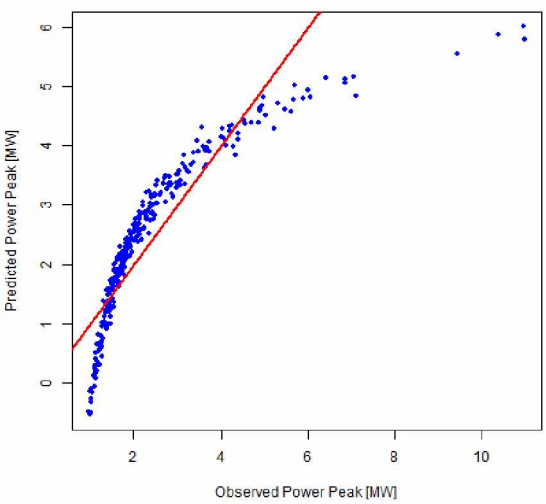

Figure 14: Comparison of the simulator outputs and the regression predictions (15% CH)

As a consequence, we have considered a nonlinear model using an Artificial Neural Network (ANN, Hopfield 1982). An ANN consists of a group of simple processing units, called basic artificial neurons, which communicate by sending signals to each other over a large number of weighted connections. They perform a relatively simple job: reception of an input signal (from neighbor or external source) and computation of an output signal which is propagated to other neurons. A basic artificial neuron is actually a non-linear function of N inputs X_i associated with their own weights W_{ij}. The weighted sum of the inputs composes the activation value (or potential) V_j. Then, a transfer function F, called activation function of the neuron, produces the output (the activation signal) from the potential signal V_j.

$$Y_j = F(V_j) = F\left(\sum_{i=1}^{N} X_i \times W_{ij}\right) \quad (6)$$

To build a network, basic neurons are organized in a particular architecture which consists of a description of the number of layers, the number of neurons in each layer, the activation functions and the connection process. The layer that produces the network output is called the output layer, and all other layers are called hidden layers (hidden neurons play an internal role in the network). Each layer has a weight matrix, an output vector, and an activation function (generally a sigmoïd for hidden layers and linear for the output layer). A huge number of architectures exist (Adaline, Radial Basic Functions, Hopfield, Kohonen, recurrent network of Jordan …), but the most common ANN model is the Multi-Layer Perceptron (MLP). A MLP has a feed-forward structure, meaning that signals propagate strictly from inputs to outputs, in contrast with feedback structure (recurrent networks) which contains connections from output to input neurons. The behavior of the feed-forward structure is more stable.

After the architecture definition, an ANN has to be trained to do a particular job by adjusting the weights according to a learning rule. During this training phase, a neural network learns the input/output relationship such that the application of a set of inputs produces outputs closer to the desired set of outputs (targets): the MLP is trained using this type of supervised learning. Among algorithms of supervised training (Conjugate Gradient Descent, Levenberg-Marquardt, Resilient Retro-Propagation, Widrow-Hoff…), the best-known is called back-propagation: input vectors and the corresponding target vectors are repeatedly presented to the neural network. The ANN output is compared to the desired output and an error is computed. The criterion used to measure to proximity of the neural network prediction to its target is generally the Least Mean Squares method. This

prediction error is then back-propagated to the neural network, and used to adjust the weights in order to minimize the error.

Finally, the major problem with training algorithms is the over-fitting (or over-learning). To limit the over-fitting, it's necessary to find a compromise between learning and generalization performances. The method of degradation of the weights ("weight decay") is a technique of regularization (or stabilization) allowing to avoid the problems of over-fitting connected to an abundance of parameters (neurons of the hidden layer). It consists in adding a penalty to the error function E to limit the combinations of parameters giving a too complex network.

In this work, we used as network a perceptron constituted by 1 hidden layer and 10 neurons (131 weights), trained with back-propagation algorithm and a weight decay of 5.E-4 on 2,000 iterations. The number of neurons to be considered for this hidden layer was optimized by analysis of error (RMSE, Root Mean Squared Error) curves. The corresponding results (Figure 15) are satisfactory because points are very well distributed around the first bisector:

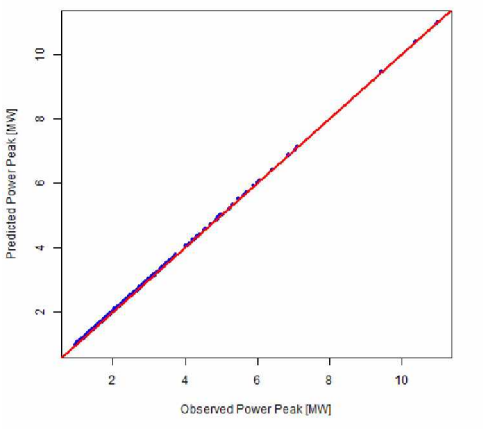

Figure 15: Comparison of the simulator outputs and the ANN predictions (15% CH)

The response surface constructed using the artificial neural network has been used to classify the most important parameters: again D1 and Abs_1, Table 6.

Table 6: Sobol' indices (total-order) for most influent input parameters (case 15%)

Power Peak	**Sobol' indices**
D1	62,6
Abs1	29,3
NuSigf1 x5	1,3
Scattering 1->2	0,5
NuSigf2	0,1
Beta 4	0,1

The same trends, as in the case of 12%, are observed during the transient (Figure 16), except for some secondary input parameters:

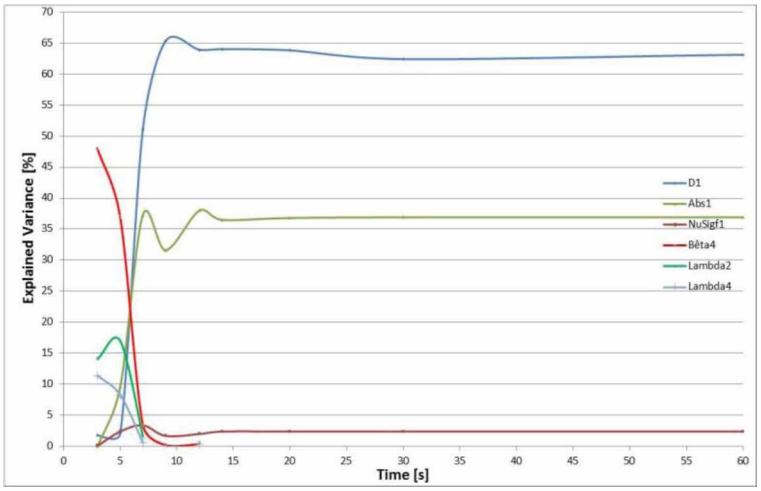

Figure 16: Time evolution of Sobol' indices (total-order) for each input parameters (15% CH)

4.2.3 Comments

Both direct and indirect techniques revealed that the dominant contributions to uncertainties of a transient peak-of-power were from the diffusion coefficient (D1) and the absorption cross section (Abs_1) of the first group. They indicate with evidence that major contribution in uncertainty comes from the terms of moderation, elastic and inelastic scattering. This is due to the simultaneous influence of their weight in the variability of the rod worth (the sensitivity coefficient) and the value of their standard deviations. This conclusion seems to be independent of the mean power peak value. Using the indirect method (a surrogate model) we show how these two XS reach their maximum influence at the moment of the power peak and they remain constant in the following.

4.3. Inverse problem – unfolding of uncertainties

Propagation of uncertainties on peak-of-power and power distribution makes sense for design optimization and, to a certain extent, for safety assessment. At the same time, it would be possible to unfold partial contributions of different macroscopic cross sections and to provide a ranking table for needed improvement in pure nuclear data. In this way, we could contribute to the programming of dedicated basic researches including experimental studies.

More explicitly, the idea we want to express is:

- The ranking of the importance of the uncertainty of an isotope is usually made as regards to the influence it has on a k effective or an assembly power peak uncertainties. That means being only interested in a steady-state and, implicitly, to assume that what it is important for a steady-state is important for a transient as well.
- We defined an 'indicator' (product of the cross section standard deviation times the absolute value of a sensitivity coefficient) which gives us the right hierarchy of cross sections in terms of their importance on the variance of the power. So, if we would to rank the 'weight' of an isotope on the power peak uncertainty, we should know the 'weight' of this isotope as regards to this indicator. And the ranking of a list of isotopes as regards to a transient could be different from a list for a steady state, even if most of the isotopes will probably be in common between the steady and the transient state;
- In this exercise, we performed a rod ejection and found that the fast diffusion coefficient and the fast absorption are the main cross sections responsible for the uncertainty of the peak power. In another type of transient other cross sections and other isotopes may be more

important. A ranking list for each transient could suggest where to improve uncertainty of the cross sections of an isotope to better compute a transient.

Vanhanen (Vanhanen et al., 2015) attempted to rank the uncertainty of the microscopic cross sections of an isotope relative to the uncertainty of homogenized and condensed macroscopic cross sections on an assembly. In this paper, an analysis is made of the capability of three major Nuclear Data Libraries (ENDF/B-VII, JEFF 3.2, JENDL-4) to generate the assembly cross section uncertainties starting from every library microscopic variance-covariance data. The computations were made using CASMO-4 and the first-order perturbation theory for, unfortunately, only a few nuclides. They associated, as major contributors to the macroscopic uncertainty, the elastic processes of the ^{16}O, the elastic and inelastic scattering of the ^{238}U to the 1st group diffusion coefficient and the ^{238}U resonance capture to the 1st group absorption

Although the results of Vanhanen were computed for different than our configurations, they confirm our observation of the "fast" group dominance over the total uncertainties in a transient simulation.

4.4. Comments to ratio Standard Deviation vs Power Peak

We have seen that the maximum standard deviation is at the moment of the power peak and it is worth, approximatively, 1.4% of the mean peak. The question, now, is to verify if this value of 1.4% is independent of the power peak value or if it changes when the power peak changes.

To verify this point, we have done a lot of other sequences of rod ejections increasing the ejection distance: from 12% to 15% Core Height (CH). A 'sequence' is an ejection characterized by the ejection distance, in percentage of CH; we have a sequence for 12%, 13%, 14%, 14.25%, 14.50%, 14.75%, 14.93% and 15% CH. The number of rod ejections for each sequence was variable due to the necessity to 'stabilize' the mean power peak.

In Figure 17 we plotted all the power peaks for each sequence (ordinate). In abscissa, the ejection calculations are ordered in ascending order (from 1 to the final number for each sequence). The same rod ejection 'm' of each sequence makes use of the same cross sections and the only difference between all the power peaks of the same 'm', is the rod ejection height.

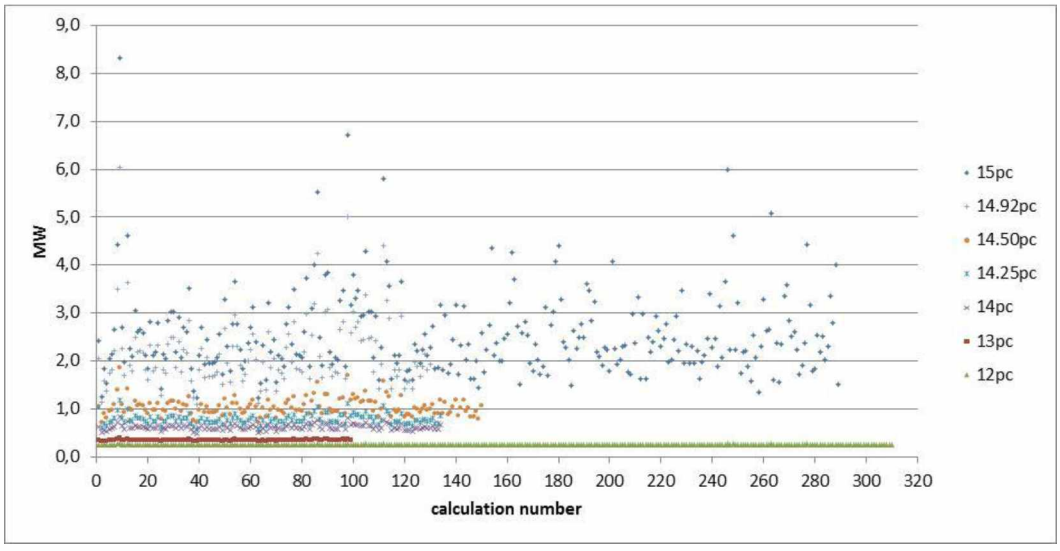

Figure 17: Power Peaks by Rod Ejection Height (Xpc = ejection distance equal to X % Core Height)

It is easy to see that, as the maximum rod ejection height increases (as a result, also the power peak) the dispersion of the results also increases. The green line (the lowest line, practically a straight line with this scale) corresponds to the benchmark specifications (12% CH) while the highest dots cloud corresponds to 15% CH.

The computed results of sampling have been translated in the curves presented in Figure 18a and b: The curve 18a shows the dependence of the standard deviation vs the mean power peak for each rod ejection core height, while the curve 18b depicts the grow rates of the dispersion and power for one of the calculated sequences.

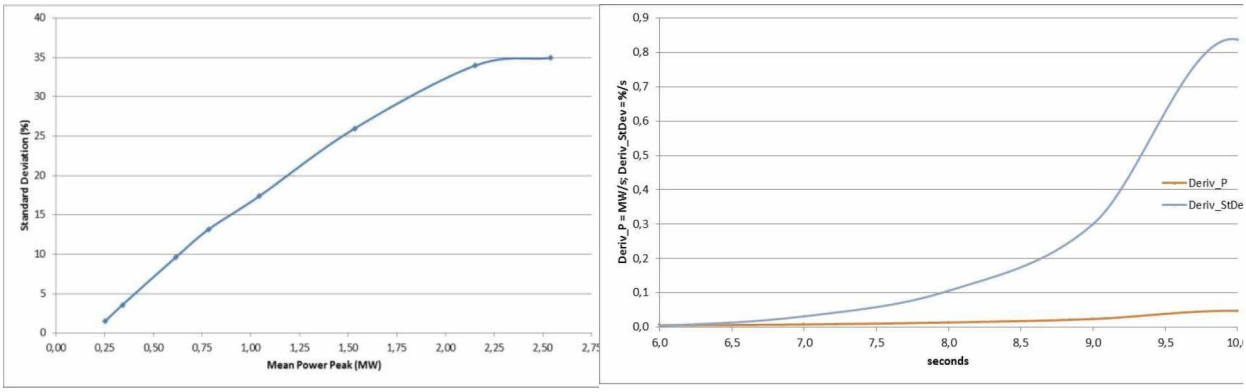

a b

Figure 18: (a) Standard Deviation (%) vs the Power Peak Mean Value and (b) Mean Power (red) and Standard Deviation (blue) derivatives vs time

The saturation effect presented in Figure 18a demonstrates that propagated uncertainty would be a function of two variables: the peak-of-power and the XS standard deviation. It also confirms that a very popular approach based on linearized sensitivity coefficients might be sometimes insufficient for a transient analysis.

Figure 18b allows seeing that the rate of a growing of dispersion exceeds one for the power at least before the peaking value (9.2÷9.3 seconds).

The only difference between an ejection up to 12% CH and an ejection up to 15% CH was the speed of the rod ejection since the time of ejection (10 seconds) was keeping constant. To check the impact of changing the rod ejection speed on the power peak standard deviation, we reduced the ejection time from 10 s to 8 s. In this way, the rod ejection speed of the case 12%-8s is the same as in the case 15%-10s. Table 7 presents the results.

Table 7: Test on the rod ejection speed

Standard Deviation (% mean power peak)	**12% core height**	**15% core height**
Ejection time = 10 sec.	*1,5%*	*32%*
Ejection time = 8 sec.	*1,4%*	*24%*

We always find an increase in the standard deviation increasing the ejection height (i.e., the power peak), even with the change of the speed. The increase of the standard deviation with the increase in

power peak does not, therefore, seem to depend on the ejection speed of the rod. This conclusion is interesting because it seems to show that, to assess the spread of uncertainty (at least for this benchmark), it is not sufficient to examine only a particular case, but it is necessary to analyze a wide range of possible cases.

5. CONCLUSIONS

The paper presents the results obtained in the framework of UAM-LWR benchmark, particularly on an exercise II-2b devoted to a propagation of few group cross sections uncertainties through a rod-ejection driven transient w/o feedback. The specification of the benchmark exercise comprises a model of so-called mini-core, a set of postulated relative standard deviations of few-group cross sections and one control rod ejection scenario without feedback. The scenario presumes one rod ejection on 12% of the core height in 10 seconds and, then, the rod return to its initial position in 20 seconds. The computation is pushed up to 60 seconds. Steady-state core power was 0.1409 MW. As said, no feedback and other physics were considered.

The studies were aimed to analyze a consistency of some uncertainty propagation methodologies for spatial and time evolution of neutron field. The exercise has been considered as a first step toward fully coupled multi-physics modeling. One should note that the latest one, in its order, requires an enhanced robustness of each single-physics module. As such robust single-physics module in our case one could take a three-dimensional, few group, and elliptic equation solver which we examined over here with respect to its suitability for an uncertainty propagation process.

To reach the statistically significant results we performed 300 runs obtaining a mean power peak around 0.25 MW with a relative standard deviation of, nearly, 1.5%. It has been observed that the time-dependent curve of the standard deviation follows the time-dependent evolution of the mean power. It is easy to see that an impact on a total power peak uncertainty due to the fast component of diffusion coefficient dominates over all others being about 2.5% and less than 1%, respectively.

Following the results and discussions given above one may summarize the following statements.

- The normal distributions of sources of uncertainty have been presumed. The question arisen in such a context is how far an inclination on normality will impact an outlined power peak uncertainty, if it will?

Trying to address this question we defined an empirical cumulative distribution function, at different moments during the transient, and we compared it to true normal and log-normal distributions. The power peaks have had normal distribution until they were close to the initial value of power. The growing of a power excursion led distributions of peaks became closer to a log-normal one; which is, however, also of high entropy that corresponded to our hypothesis.

- Does it exist and, if yes, which relationship would be between the mean power peak and its relative standard deviation.

According to our numerical studies, one may state that a relative standard deviation increases together with a mean peak value. It seems reasonable to take into account this effect in a process of uncertainty propagation especially in case of scaling of uncertainties.

- How to quantify impacts due to each particular nuclear reaction in the total uncertainty and which one dominates over others and why.

To identify the most impacting XS we were repeating the transients and plotting the ratios between the partial variance, due to a given cross section, and the total variance. The results demonstrated the dominance of the uncertainties of the diffusion coefficient and absorption cross sections in the fast group (D1 and Abs_1). Trying to ensure ourselves that it is so, we computed sensitivities of rod worth to cross sections variations. Its dot product with relevant uncertainties of XS confirmed the results after the sampling. Then scaling analysis has been performed, where we increased the rod ejection height, repeated the computations and obtained a power peak ten times higher than in the benchmark, with the same conclusions concerning the most impacting cross sections. Similar results have been obtained using a Sobol' analysis.

The following suggestion could be stated in such a context.

- Since a standard deviation of the fast diffusion coefficient, among others, has the strongest influence on power variability one could suggest to make this source of uncertainty as low as possible.

A reduction of uncertainties always means an improvement of knowledge about the physics behind the data. The last one requires, at least, two the following steps: (1) an identification and a prioritization of the most impacting nuclide-reaction channels in terms of their contributions in the fast diffusion coefficient, as such, and, then, (2) an addressing these issues to nuclear data evaluation community. So, one could suggest an unfolding of uncertainties in order to considering our results as relevant inputs stimulate an establishment of theoretical and experimental problem-oriented basic researches.

- It is easy to see that, in our power excursion calculations, the relative standard deviation grows faster than the power itself. One could suggest take these phenomena into account scaling transients and relevant uncertainties.

- We suggest paying attention to a transposition of values and associated uncertainties estimated for steady-state conditions, on transients.

For example, a conservative approach uses to be based on the "most penalizing" scenarios verifying, in such a way, whether or not all safety criteria are satisfied above any reasonable doubts. But such conservatism being established for the steady-state configurations, would be inadequate for transient ones. So we suggest establishing so-called informed conservative assumptions for each given transient, or to each given family of transients, being warranted that sometimes even small changing of the conditions or the transient sequences could result in a significant change of uncertainties and biases.

Finally, one should note that the exercise, as such, and its results are considered only as a first phase in an analysis of uncertainty propagation capabilities for existing design oriented multi-physics tools and in a characterization of relevant safety margins. In such a case even this rough analysis where all feedback were missed and uncertainties' representation was simplified so far looks, nevertheless, appropriate being at the same time an important milestone in a long comprehensive research program.

REFERENCES

K. Ivanov, M. Avramova, "Chapter 10: LWR — Reactivity Transients and Accidents", in Modern Nuclear Energy Analysis Methods; Design-Basis Accident Analysis Methods for Light-Water Nuclear Power Plants, pp. 411-496 (2019)

J. Hou et al., 'Benchmark for Uncertainty Analysis in Modelling (UAM) for Design, Operation and Safety Analysis of LWR, Phase II', NEA/NSC/DOC(2014), April 2017

UAM-XS, 2014. https://www.oecd-nea.org/science/wprs/egrsltb/UAM/index.html

F. Barré, C. Grandjean, M. Petit, and J-Ce Micaelli, "Fuel R&D Needs and Strategy towards a Revision of Acceptance Criteria,", *Science and Technology of Nuclear Installations*, vol. 2010, Article ID 646971, 7 pages, 2010. https://doi.org/10.1155/2010/646971.

M. Hursin, T. J. Downar, R. Montgomery, 'Impact of improved neutronic methodology on the cladding response during a PWR reactivity initiated accident', *Nuclear Engineering and Design*, **262**, 2013, Pages 180-188,

B. Miglierini, T. Kozlowski, Vit Kopecek, Uncertainty analysis of rod ejection accident in VVER-1000 reactor, *Annals of Nuclear Energy*, Volume 132, 2019, Pages 628-635,

D.F. da Cruz, D. Rochman & A.J. Koning, 'Propagation of nuclear data uncertainty for a control rod ejection accident using the total Monte-Carlo method', *PHYSOR 2014 - The Role of Reactor Physics toward a Sustainable Future*, Kyoto, Japan, September 28 - October 3, 2014

Diamond,D.J., Aronson,A., And Yang,C. A QUALITATIVE APPROACH TO UNCERTAINTY ANALYSIS FOR THE PWR ROD EJECTION ACCIDENT. United States: N. p., 2000. Web.

A. Sargeni, F. Fouet, E. Ivanov, P. Probst, 'An IRSN Contribution to the UAM Project: Mini-Core, Numerical Rod Ejection Exercise', *PHYSOR 2018*, Cancun, Mexico, Avril 2018

M. Avramova, K. Ivanov, 'Verification, Validation and Uncertainty Quantification of Multi-physics Modeling of Nuclear Reactors', Elsevier Science Publishing Co Inc, Woodhead Publishing Series in Energy, 2020

Ryan N. Bratton, M. Avramova, K. Ivanov, 'OECD/NEA benchmark for uncertainty analysis in modeling (UAMfor LWRS – Summary and discussion of neutronics cases (Phase I), *Nuclear Engineering and Technology*, **46**, Issue 3, 2014, Pages 313-342, ISSN 1738-5733, https://doi.org/10.5516/NET.01.2014.710.

F. Dubois, B. Normand, A. Sargeni, 'An example of Neutronic penalizations in reactivity Transient Analysis Using 3D Coupled Chain HEMERA", *Physor 2012*, April 15-20, 2012, Knoxville, Tennessee, USA

J.J. Lautard, S. Loubière, C. Maganud,'CRONOS, A Modular Computational System for Neutronics Core Calculations', *IAEA Specialists Meeting*, France, September 1990

R. Sanchez, I. Zmijarevic et al, 'APOLLO2 Year 2010', *Nuclear Engineering and Technology*, **42** (5), October 2010

M. Salvatores, G. Palmiotti, G. Aliberti, P. Archier, C. De Saint Jean, E. Dupont, M. Herman, M. Ishikawa, T. Ivanova, E. Ivanov, S.-J. Kim, I. Kodeli, G. Manturov, R. McKnight, S. Pelloni, C. Perfetti, A.J.M. Plompen, B.T. Rearden, D. Rochman, K. Sugino, A. Trkov, W. Wang, H. Wu, W.-S. Yang, 'Methods and Issues for the Combined Use of Integral Experiments and Covariance Data: Results of a NEA International Collaborative Study', *Nuclear Data Sheets*, **118**, 2014, Pages 38-71

N. Leclaire, T. Ivanova, E. Letang, E. Girault, J.F. Thro, 'Fission product Experimental Program : Validation and Computational Analysis', *Nuclear Science and Engineering*, 161-2, 2009, Pages 188-225

Xinyi Pan, Bin Jia, Jingru Han, Jianping Jin, Chunming Zan, 'Systematic and quantitative uncertainty analysis for rod ejection accident of pressurized water reactor', *Energy Procedia*, **127** (2017), 369-376

I.M. Sobol', 'Sensitivity estimates for nonlinear mathematical models'. *Mathematical Modelling and Computational Experiments*, 1, pp. 407–414 (1993).

D. Rozon (1992), "Introduction à la cinétique des réacteurs nucléaires", Ecole Polytechnique de Montréal, ch. 3

C. Mesado, A. Soler, T. Barrachina, et al., "Uncertainty and Sensitivity of Neutron Kinetic Parameters in the Dynamic Response of a PWR Rod Ejection Accident Coupled Simulation,", *Science and Technology of Nuclear Installations,* vol. 2012, Article ID 625878, 10 pages, 2012. https://doi.org/10.1155/2012/625878.

M. Pusa, 'Perturbation-Theory-Based Sensitivity and Uncertainty Analysis with CASMO-4', *Science and Technology of Nuclear Installations*, Volume 2012, Article ID 157029, (2012)

N.A. Butler, 'Optimal and orthogonal Latin hypercube designs for computer experiments', *Biometrika*, 88, 3, pp. 847-857 (2001).

J.J. Hopfield, (1982), "*Neural networks and physical systems with emergent collective computational abilities*", Proceedings of the National Academy of Sciences, **79**, 2554-2558. Reprinted in Anderson and Rosenfeld (1988).

R. Vahanen, M. Pusa, 'Survey of prediction capabilities of three nuclear data libraries for a PWR application', *Annals of Nuclear Energy*, **83** (2015), 408-421